Effect of microtubule-targeting drugs on cell–cell and cell–matrix junctions in tumor epithelial cells

Laura Tonutti[a], Elena Bononi[a], Luca Paris[a], Fabienne Breillout[b], Nathalie Corvaia[c], Christian Bailly[c] and Gianfranco Bazzoni[a]

In this study, we investigated the effects of microtubule-targeting drugs, which either destabilize (the Vinca alkaloid vincristine) or stabilize (the taxane derivative docetaxel) microtubules, on the cell–cell and cell–matrix adhesive junctions of Caco-2 tumor epithelial cells, using fluorescence imaging and functional assays. We found that, in sub-confluent (but not confluent) cells, vincristine (but not docetaxel) affected cell–cell junction morphology. Furthermore, docetaxel (but not vincristine) attenuated the formation of the peri-junctional actomyosin ring and enhanced the internalization of junctional adhesion molecule-A. However, these effects of vincristine and docetaxel did not translate into appreciable functional changes during the opening and resealing of the cell–cell junctions. We also found that vincristine caused enlargement of focal adhesions (the major cell–matrix junctions) without affecting cell adhesion onto the matrix. Thus, we conclude that the microtubule-targeting drugs interfere to variable degrees with the morphology and/or function of the cell–cell and cell–matrix adhesive junctions. In addition, the results highlight the importance of considering the cellular context and dynamics (e.g. cell confluence and junction opening, respectively), when determining the final effects of microtubule manipulation on cell adhesiveness. *Anti-Cancer Drugs* **22:234–244**

Anti-Cancer Drugs 2011, **22**:234–244

Keywords: Caco-2 cells, cell adhesion, epithelial cells, microtubules, taxoids, Vinca alkaloids

[a]Mario Negri Institute of Pharmacological Research, Milano, Italy, [b]Pierre Fabre Oncologie, Boulogne and [c]Centre d'Immunologie Pierre Fabre, St Julien-en-Genevois, France

Correspondence to Dr Gianfranco Bazzoni, MD, Department of Biochemistry and Molecular Pharmacology, Istituto di Ricerche Farmacologiche Mario Negri, via La Masa 19, I-20156 Milan, Italy
Tel: +39 02 39014480; fax: +39 02 39014744;
e-mail: gianfranco.bazzoni@marionegri.it

Received 13 October 2010 **Revised form accepted** 27 November 2010

Introduction

Normal cells adhere to the neighboring cells through cell–cell junctions, such as tight junctions [1], adherens junctions [2], and desmosomes [3], which together form the junctional complex (JC). In addition, they adhere to the extracellular matrix through cell–matrix junctions, such as focal adhesions (FA) [4]. In contrast, in transformed cells, junctions undergo profound changes [5,6], which is thought to facilitate cell detachment from the primary tumor, local invasion, and metastatic spreading. Thus, understanding the mechanisms that underlie junction regulation should facilitate the identification of key targets for anticancer drugs. Among such mechanisms, putative connections link junctions (both JC and FA) and microtubules (MT), which is particularly promising, because MT-targeting drugs are available for clinical use.

Three molecular pathways are potentially concerned (Fig. 1a). First, MT disassembly releases the rho activator GEF-H1 [7], thus leading sequentially to activation of rho and rho-kinase, inactivation of myosin light chain-specific phosphatase, increased levels of phosphorylated myosin light chain [8], contraction of the peri-junctional actomyosin ring [9], and traction on the JC [10]. Second, MT disassembly releases kinesins, thus predictably impairing the kinesin-mediated delivery of proteins to both cell–cell [11] and cell–matrix [12] junctions, which (assuming that internalization is not concomitantly decreased) should reduce the surface levels of JC and FA components [13]. Third, MT disassembly releases MT-associated LIM kinases, which causes sequential inhibition of the actin-severing protein, cofilin, enhanced formation of actin stress fibers [14], and traction on the FA [15]. Thus, as a net result, MT disassembly is expected to interfere with the JC and FA and ultimately to weaken cell attachment to both neighboring cells and extracellular matrix.

Representing signaling events as linear pathways that impact on functional responses (as shown in Fig. 1a) may suggest that drugs specific for key cellular targets should invariably inhibit a given response. However, the identification of specific drug-target–response connections is challenging, because of the limitations in our knowledge of the signaling pathways, and of the biochemical and biophysical mechanisms whereby signals are initially relayed to structural molecules (e.g. phosphorylation of cytoskeletal proteins) and subsequently translated into functional responses (e.g. generation of contractile forces). In addition, even a single molecular perturbation often activates multiple pathways, thus possibly eliciting more than one response. Finally, the same signal may induce different responses depending on the cellular context and on the dynamics of the biological process under scrutiny [16]. As a consequence, pharmacological interventions (no

0959-4973 © 2011 Wolters Kluwer Health | Lippincott Williams & Wilkins DOI: 10.1097/CAD.0b013e3283432479

Fig. 1

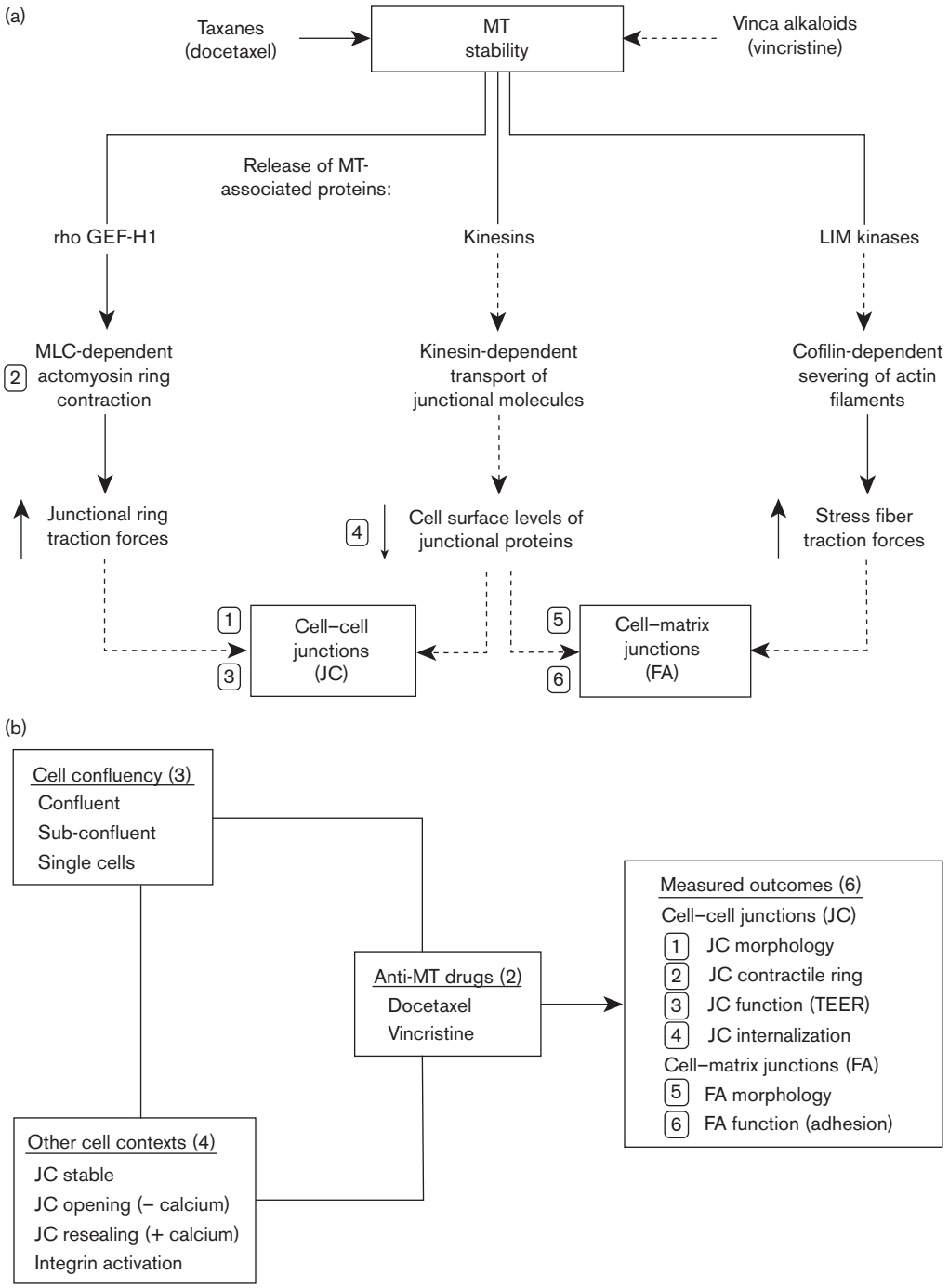

Microtubule (MT)-targeting drugs and cell junctions. In (a), the mechanisms that link MT and junctions are schematically represented. Solid and dotted lines indicate positive and negative effects, respectively. In (b), the experimental design is shown. FA, focal adhesions; JC, junctional complex; MLC, myosin light chain; TEER, transepithelial electrical resistance.

matter how specifically targeted against a given molecule) usually impact on complex networks of interconnected pathways and often with unpredictable outcomes [17].

Here, to examine the pharmacological modulation of the connection between MT and junctions in a reasonably broad context, we have undertaken a multiparametric study. As summarized in Fig. 1b, we have treated tumor epithelial cells with two prototype MT-targeting drugs. Further, we have performed experiments in different cellular contexts (e.g. confluent versus sub-confluent cells) and dynamics (e.g. junction opening versus resealing).

Finally, we have measured six outcomes that reflect morphological and functional changes in the cell–cell and cell–matrix junctions. Even though we have selected a limited number of drug-context–outcome combinations, the approach has highlighted interesting combinations (e.g. sensitivity of the junctions to MT disassembly in sub-confluent cells) and an unanticipated robustness of cell adhesion even in the face of a strong pharmacological perturbation of the MT-based cytoskeleton.

Methods

Immunofluorescence microscopy

Epithelial Caco-2 cells (from human colon carcinoma) were cultured in Dulbecco's modified Eagle's medium (D-MEM; Gibco, Invitrogen Corporation, Carlsbad, California, USA) supplemented with 20% fetal bovine serum (Sigma, St Louis, Missouri, USA). To obtain confluent and sub-confluent cells, the cells were seeded onto glass cover slips at different densities (1.5 and 0.4×10^5 cells/cm^2, respectively) and grown for different times (72 and 48 h, respectively). Then, the cells were incubated (for 60 min at 37°C) with either medium alone or the drugs. The cells were fixed with 3.7% paraformaldehyde, permeabilized with 0.5% Triton-X-100, and blocked with 1% bovine serum albumin (for 15, 3, and 60 min, respectively). The cells were stained with primary antibodies [mouse anti-α-tubulin monoclonal antibody (mAb) B-5-1-2, Sigma; mouse anti-vinculin mAb hVIN-1, Sigma; rabbit anti-zonula occludens-1 (ZO-1) serum (Zymed, San Francisco, California, USA)] and secondary antibodies (rhodamine-conjugated anti-mouse and anti-rabbit IgG, Jackson, West Grove, Pennsylvania, USA). Finally, cover slips were mounted in 488-Mowiol and analyzed with a fluorescence microscope [18,19].

The peri-junctional actomyosin ring was examined as follows. In brief, to deplete extracellular calcium (and induce formation of the ring), confluent Caco-2 cells were incubated (for 60 min at 37°C) with calcium-free Spinner modification of the minimum essential medium (S-MEM) in either the absence or presence of the drugs. Then, to restore calcium, the cells were incubated with D-MEM (for 60 min). Finally, the cells were fixed and stained with fluorescein isothiocyanate-conjugated phalloidin (Alexis, Plymouth Meeting, Pennsylvania, USA).

Transepithelial electrical resistance

Caco-2 cells were plated (in 12-well plates) on transwell polyester filters, with a pore size of 0.4 μm and a diameter of 12 mm (Costar Corporation, Lowell, Massachusetts, USA). In some experiments, for measuring dynamic changes in transepithelial electrical resistance (TEER) on cell–cell junction opening and resealing, the cells were treated (for 20 min at 37°C) with 2 mmol/l of ethylene glycol tetra-acetic acid (EGTA; in PBS without divalent cations), to induce junction disruption. Then, fresh medium was added back, to induce junction resealing, as described [20]. Before each TEER measurement, the culture medium was replaced with fresh medium. Then, TEER was measured (with a Millicell-ERS device, Millipore Corporate, Billerica, Massachusetts, USA) by averaging two measurements in each filter, subtracting the blank value, and multiplying the result of the subtraction by the effective surface area of the filter membrane (1.12 cm^2). TEER values are expressed as Ω cm^2.

Internalization by fluorescence microscopy and flow cytometry

For fluorescence microscopy, Caco-2 cells were seeded onto glass cover slips (at a density of 1.5×10^5 cells/cm^2 in 24-well plates) and grown to confluence for 3 days. Then, the cells were incubated (at 37°C for 60 min) in either the absence or presence of the drugs (in complete culture medium). After one wash with washing buffer (ice-cold PBS with calcium and magnesium), the cells were incubated (for 45 min on ice) with mouse anti-junctional adhesion molecule-A (anti-JAM-A) mAb BV16 (Hbt, Uden, the Netherlands). After three washes, the cells were incubated (for 45 min on ice and protected from light) with a rhodamine-conjugated IgG antiserum (all antibodies were dissolved in cold washing buffer). After three washes, the cells were treated with cold D-MEM (plus 20% serum). Then, the plates were incubated for 45 min at either 37 or 4°C (to allow and prevent internalization, respectively). After one wash, the cells were treated twice for 2 min with either cold antibody-stripping buffer (150 mmol/l of NaCl, 50 mmol/l of glycine) at pH 2.5 (to remove surface-bound antibody) or cold washing buffer. Finally, the cells were washed, fixed with 3.7% paraformaldehyde, and analyzed by fluorescence microscopy.

For flow cytometry, the cells were seeded in six-well culture plates, at a density of $4–9 \times 10^4$ cells/cm^2, and grown to confluence. Then, the cells were treated as described above, except that the antibodies were diluted in cold culture medium plus serum, and that the cells were stained with a fluorescein isothiocyanate-conjugated secondary antibody. Subsequently, the cells were detached with cold trypsin, suspended with cold D-MEM, and kept on ice. Cell suspensions were centrifuged, washed, fixed with 1% paraformaldehyde, and analyzed by flow cytometry.

Cell–matrix adhesion assay

96-well plates were incubated (overnight at 4°C) with either fibronectin (dissolved in Tris-buffered solution; TBS) or TBS alone (blank). Next, the wells were washed with TBS and incubated (for 60 min at 37°C) with 0.1% heat-inactivated bovine serum albumin, to block non-specific binding sites. In parallel, suspensions of Caco-2 cells were labeled with the fluorescent marker, 2′,7′-bis-(2-carboxyethyl)-5-(and-6)-carboxyfluorescein-acetoxymethyl ester (Sigma) during a 30-min incubation (at 37°C) with labeling buffer (Roswell Park Memorial Institute medium

containing 10 mmol/l of Hepes, 0.1% albumin, and 5 μg/ml of 2′,7′-bis-(2-carboxyethyl)-5-(and-6)-carboxyfluorescein-acetoxymethyl ester). Then, the labeled cells were washed three times with TBS, suspended in assay buffer (TBS containing 0.1% albumin and 2 mmol/l of glucose) and treated in either the absence or presence of manganese chloride and the drugs. Subsequently, 50 000 cells were added to each well, and allowed to adhere by means of incubation for 60 min at 37°C. At the end of the incubation, the wells were washed three times with warm TBS, to remove all nonattached cells. Then, the fluorescence of each well was measured with a microplate reader and normalized by subtracting the average fluorescence of the blank wells [21]. Finally, the number of adherent cells per well was determined with the linear part of a calibration curve, using PRISM 2.0 (GraphPad Software, Inc., La Jolla, California, USA).

Results

Vincristine (but not docetaxel) affects cell–cell junction morphology in sub-confluent cells

We first used fluorescence microscopy to analyze the effects of treating Caco-2 cells with vincristine and docetaxel (10 μmol/l each, for 60 min) on cell–cell junctions. We focused initially on sub-confluent cells, which form partially mature junctions, and found that vincristine caused morphological changes. Specifically, while in control-treated and docetaxel-treated cells the staining of the tight junction molecule ZO-1 was linear and continuous, in vincristine-treated cells ZO-1 staining was more irregular and discontinuous. In some cells, the ZO-1-based junctions seemed to be delaminated (Fig. 2, first row). Interestingly, the effect of vincristine resembled the effect of the calcium-free medium S-MEM (second row), which causes junction disassembly, thus reinforcing the link between MT and junction stability.

However, when analyzing confluent cells, which form more mature junctions, we found that, in docetaxel-treated and vincristine-treated cells, the staining of ZO-1 (third row) was unaffected. As a control, we confirmed that both drugs were effective on MT regardless of the degree of cell confluence. Specifically, in both sub-confluent (not shown) and confluent (fourth row) cells alike, MT seemed to be thicker in docetaxel-treated cells and more disorganized in vincristine-treated cells, compared with control-treated cells. We thus hypothesized that the ability of vincristine to selectively affect cell–cell junctions in sub-confluent (but not confluent) cells might reflect the presence of more stable cell–cell junctions in confluent cells, which led us to investigate the junction dynamics.

Docetaxel (but not vincristine) interferes with junctional contractility

Conceivably, the assembly of junctions and MT contributes to cell–cell cohesion, which opposes cell retraction. Conversely, the disassembly of junctions and MT induces a contractile peri-junctional actomyosin ring, which favors cell retraction [22]. Here, depletion of extracellular calcium (with S-MEM) was used to induce junction disassembly and ring formation, whereas calcium restoration (with D-MEM) was used to reverse both responses [23], with the aim of testing whether the MT-targeting drugs might interfere with junction dynamics.

Under control conditions (D-MEM), actin was organized as stress fibers and cortical filaments (Fig. 3a, panel i). This type of actin distribution was unaffected in vincristine-treated (panel ii) and docetaxel-treated (panel iii) cells. Then, after junction disassembly (S-MEM), the cortical actin filaments reorganized into peri-junctional rings with radiating cables (panel iv). Of note, although vincristine (panel v) did not affect the rings and cables, docetaxel slightly attenuated the appearance of both structures (panel vi).

Next, to restore calcium, the cells were sequentially incubated with S-MEM followed by D-MEM (panels vii–ix), either in the absence or in the presence of the drugs. As a control, the cells were incubated with D-MEM followed by D-MEM (panels x–xii). Switching from S-MEM back to D-MEM reversed the effects of calcium depletion, with the nearly complete disappearance of rings and cables and with the reappearance of cortical filaments (panel vii). However, neither vincristine (panel viii) nor docetaxel (panel ix) prevented any of the changes induced by calcium restoration.

In addition, we analyzed the distribution of the junctional component JAM-A by fluorescence microscopy. Although S-MEM (but not D-MEM) induced the opening of the JAM-A-based intercellular junctions, no differences were observed among control-treated, vincristine-treated, or docetaxel-treated cells, suggesting that the effects on the actin ring and on the cell–cell junctions could be dissociated (not shown).

Neither vincristine nor docetaxel interfere with the barrier function of the tight junctions

The barrier function to paracellular permeability, which mostly relies on tight junction assembly [24], translates into the development of TEER [25]. When Caco-2 cells were grown on filters, TEER increased steadily and reached values greater than 1800 Ω cm^2 after approximately 3 weeks of culture, whereas the blank values (filters alone) averaged 160 Ω cm^2 (not shown). Then, the cells were incubated in either the presence or absence of vincristine or docetaxel (10 μmol/l for 60 min). Subsequently, the drug-containing medium was replaced with fresh medium. The TEER was measured before adding the drugs (T0), immediately after adding fresh medium (T1), and after 6 h (T2) and 72 h (T3). As shown

Fig. 2

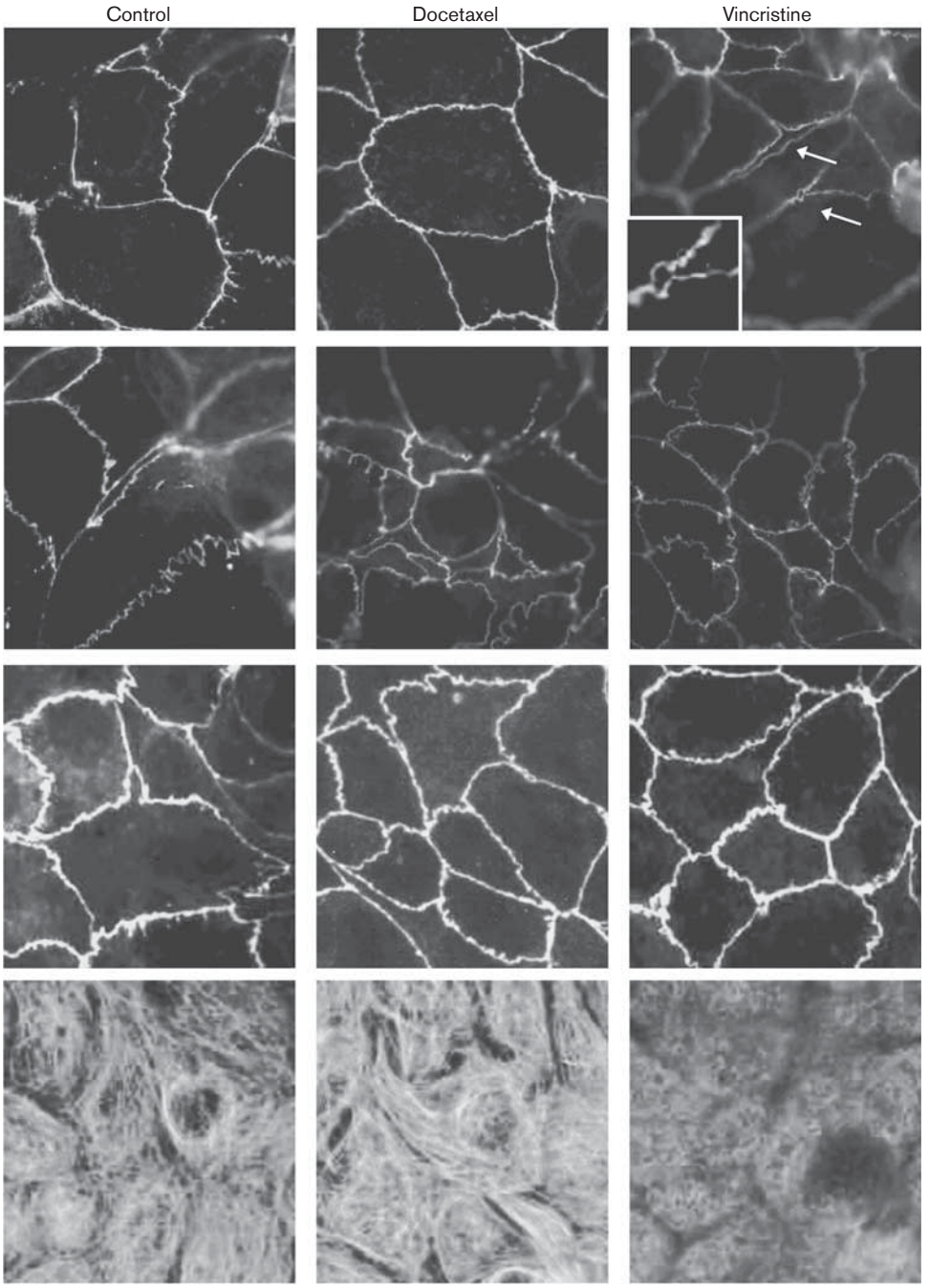

Cell–cell junction morphology. Sub-confluent (first and second rows) and confluent (third and fourth rows) Caco-2 cells were incubated (for 60 min) with either medium alone or the drugs, then fixed and stained with anti-zonula occludens-1 (first, second, and third rows) and anti-tubulin (fourth row) antibody, followed by rhodamine-conjugated anti-rabbit and anti-mouse IgG, respectively. The second row shows the effect of calcium-free medium.

in Fig. 3b (top panel), the TEER remained constant throughout the experiment and was not affected in the presence of either vincristine or docetaxel.

Next, the extracellular calcium was first depleted and then restored, to induce tight junction disruption and formation, respectively [26]. In brief, after calcium depletion with EGTA (2 mmol/l), the cells were incubated (for 60 min) with either vincristine or docetaxel, and then the drug-containing medium was replaced with fresh D-MEM. As shown in Fig. 3b (bottom panel), EGTA caused TEER to fall rapidly by more than 75% (T0

Fig. 3

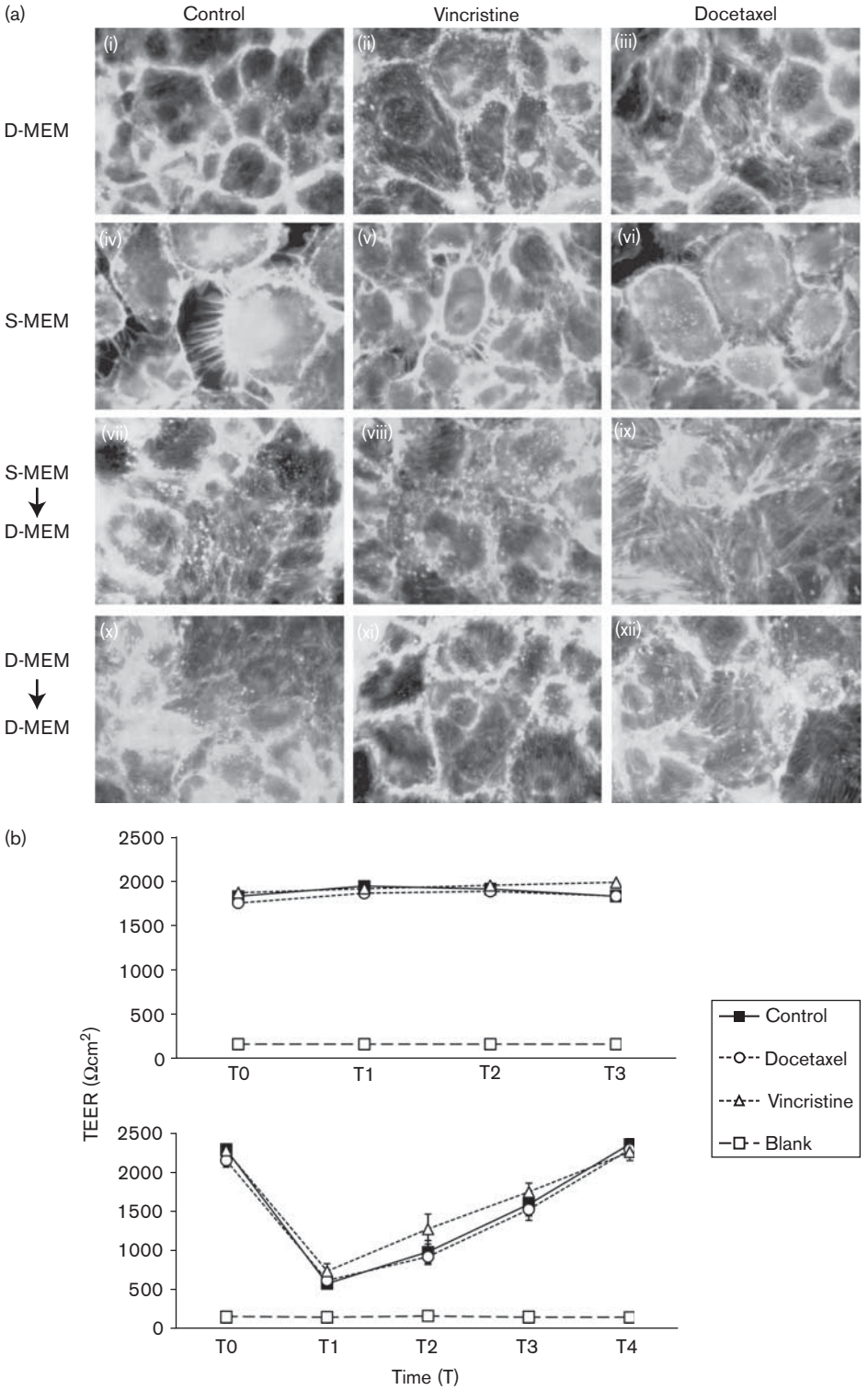

Cell–cell junction dynamics and function. (a) Confluent Caco-2 cells were incubated (for 60 min at 37°C) with either D-MEM (i–iii and x–xii) or S-MEM (iv–ix). In some experiments, cells were incubated for additional 60 min at 37°C with D-MEM (vii–xii). Then, cells were treated (for 60 min) with the drugs, fixed, stained with fluorescein isothiocyanate-conjugated phalloidin, and examined by fluorescence microscopy. (b) Caco-2 cells were grown on filters until reaching stable transepithelial electrical resistance (TEER) values (T0). Then (top panel), cells were treated (for 60 min at 37°C) with the drugs (10 μmol/l). TEER was measured 1 h (T1), 6 h (T2), and 72 h (T3) after drug treatment. Otherwise (bottom panel), cells were incubated with EGTA (for 20 min at 37°C). Finally, cells were incubated (for additional 60 min at 37°C) with the culture medium and treated with the drugs (10 μmol/l). TEER was measured immediately after calcium depletion (T1), and at 1 h (T2), 6 h (T3), and 24 h (T4) after restoring normal extracellular calcium levels. Values, which are expressed as Ωcm^2, represent mean ± standard deviation from a representative experiment.

and T1). Neither drug, however, interfered with TEER recovery, which was completed 24 h after calcium restoration (T4).

Docetaxel enhances junctional adhesion molecule-A internalization

Trafficking of junctional molecules is another mechanism of junction regulation that might be sensitive to MT-targeting drugs. For instance, MT stabilization may favor the delivery of junctional molecules to the cell surface and thus the *de novo* assembly of the junctions [23], as it was shown after the disruption of pre-existing junctions [27]. Here, we examined the constitutive internalization of the junctional molecule JAM-A. By internalization, we refer to the amount of antibody-bound antigen that becomes resistant to stripping after being internalized inside the cell (during a 37°C incubation). By fluorescence microscopy, we could confirm that, on a 37°C incubation followed by stripping, only internalized JAM-A was visible. In contrast, both junctional and internalized JAM-A were detectable on a 37°C incubation not followed by stripping. Furthermore, neither junctional nor internalized JAM-A was detectable on a 4°C incubation followed by stripping, whereas only junctional JAM-A was detectable on the 4°C incubation not followed by stripping (not shown).

Subsequently, to quantify JAM-A internalization, we measured by fluorescence-activated cell sorting analysis (FACS) the mean fluorescence intensity (MFI) of each experimental point (i.e. 37°C vs. 4°C, stripping vs. washing buffer, and absence vs. presence of the drugs). Then, for each internalization condition (i.e. incubation at 37°C followed by stripping), the MFI was normalized by subtracting the background MFI (i.e. incubation at 4°C followed by stripping) and by dividing the result by the total cell surface MFI measured before internalization (i.e. incubation at 4°C without stripping). Finally, the amount of internalized JAM-A (during a 45-min incubation) was expressed as a percentage of the total cell surface levels.

FACS analysis confirmed that a fraction of surface JAM-A was internalized, as the profile of internalized JAM-A was shifted to the left compared with the profile of total cell surface JAM-A. With either vincristine or docetaxel, the internalization curve was shifted to the left as well, indicating that JAM-A was still internalized even in the presence of the drugs. However, docetaxel increased JAM-A internalization, because the shift of docetaxel-treated cells was less pronounced compared with control-treated and vincristine-treated cells (Fig. 4). As a control, in either the absence or presence of vincristine and docetaxel, similar profiles for the total cell surface and background conditions (as defined above) were obtained.

Vincristine affects cell–matrix junction morphology but not function

Cells adhere to the extracellular matrix, in a way that depends on adhesion molecules (e.g. integrins) and FA components (e.g. vinculin). We first used fluorescence microscopy to analyze the effects of vincristine and docetaxel (10 μmol/l) on FA in Caco-2 cells that had been plated onto fibronectin. In sub-confluent cells, vinculin-based FA were small and peripheral in control-treated and docetaxel-treated cells, whereas they increased in number and size in vincristine-treated cells (Fig. 5a, panels i-iii). In contrast, in confluent cells, FA were homogeneous in size and distributed evenly, regardless of the treatment with the MT-targeting drugs (panels iv–vi).

The effect of vincristine on FA morphology led us to investigate the possible effects on cell–matrix adhesion. To this aim, we used an in-vitro adhesion assay, both under resting conditions and on stimulation with manganese, which is a known integrin activator [28]. Preliminary experiments indicated that Caco-2 cells constitutively adhered to fibronectin-coated (2.5 μg/ml) wells and that the addition of manganese chloride (0.5 mmol/l) strongly enhanced the fraction of adherent cells. Increasing the concentration of either fibronectin or manganese did not enhance any further the fraction of adherent cells. In any case, we found that neither vincristine nor docetaxel affected the constitutive and the manganese-stimulated adhesion to fibronectin (Fig. 5b).

Discussion

This multiparametric study was undertaken to evaluate the effects of a prototype Vinca alkaloid (vincristine) and a prototype taxane (docetaxel) on the cell–cell and cell–matrix adhesive junctions in tumor epithelial cells. Although the direct target of these drugs is the MT-based cytoskeleton, biochemical evidence (summarized in Fig. 1) justifies investigating their effects on indirect targets also, such as the two junctional adhesion systems. Actually, investigating the effect of MT-targeting drugs on cell adhesion is not unprecedented. To give a few examples, actomyosin ring contraction (in human SK-CO-15 colon cancer cells) was found to be sensitive to docetaxel, paclitaxel, and (albeit at higher concentrations) nocodazole [23]. Furthermore, TEER (in endothelial cells cocultured with astrocytes) was reported to decrease in response to vinblastine and (to a lower extent) paclitaxel [29]. Finally, the morphology and function of the cell–matrix FA were reported to change in cells treated with various MT-targeting compounds [30–32].

The major conclusions from this study are that vincristine and docetaxel affected (or failed to affect) a variety of adhesion-related experimental readouts and, importantly, that the final outcome depended on the general context of the cell (e.g. degree of confluence) and on the dynamics of its adhesive structures (e.g. degree of junction strength). Specifically, although the drugs induced the expected modifications in their direct target, that is, MT thickening (docetaxel) and disassembly (vincristine), these evident changes in MT were associated with changes in the two

Fig. 4

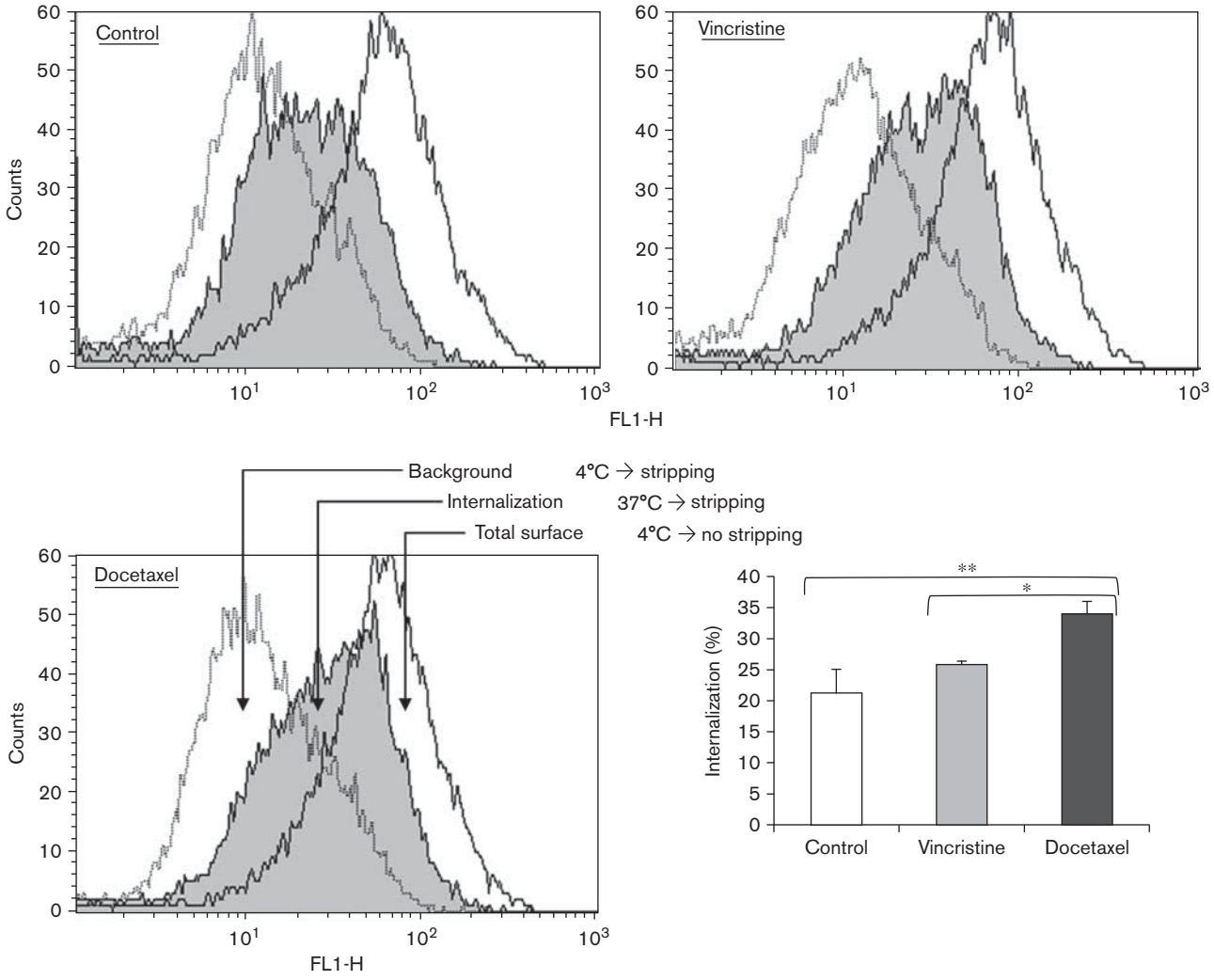

Junction internalization. Confluent Caco-2 cells were incubated (for 60 min at 37°C) in either the absence or presence of the drugs (10 μmol/l). Cell surface JAM-A was labeled (at 4°C) with anti-JAM-A monoclonal antibody BV16 followed by a fluorescein isothiocyanate-labeled secondary antiserum. Then, cells were incubated (for 45 min) at either 37°C or 4°C, to allow and prevent internalization, respectively. Surface-bound antibody was removed with an antibody-stripping buffer (pH 2.5) to detect only internalized JAM-A. Finally, cells were collected for fluorescence-activated cell sorting (FACS) analysis. Results (FACS profiles and quantification of internalization) from a representative experiment (10 000 events per sample) are shown. Data have been normalized with respect to the negative samples (i.e. treated with medium alone and stained with the secondary antibody only; not shown) and are expressed as percent of total cell surface levels. *$P<0.05$, **$P<0.01$. FL1-H, fluorescence-1 channel.

adhesion systems only under specific experimental conditions. As summarized in Fig. 6a, vincristine (but not docetaxel) affected the morphology of both cell–cell and cell–matrix junctions in sub-confluent cells, but not in confluent cells. Furthermore, docetaxel (but not vincristine) reduced actomyosin ring formation on cell–cell junction opening (but not ring disappearance on junction resealing) and increased the internalization rate of the junctional component JAM-A.

Nevertheless, despite the effect of vincristine on cell–cell junction morphology and despite the effects of docetaxel on ring formation and junctional molecule internalization, neither vincristine nor docetaxel affected the overall cell–cell adhesive function, as evaluated with measurements of stable TEER (in resting cells) and dynamic TEER (on junction opening and resealing). Similarly, in spite of the effect of vincristine on cell–matrix junction morphology, the drug did not affect the overall cell–matrix adhesive function, as evaluated in the cell adhesion assay.

To provide a schematic overview, we outlined the rules in the form of 'if, and if, then' conditional statements, which may help predict the outcome of the pharmacological modulations of MT under different conditions of cellular context and adhesion dynamics (Fig. 6b). In addition, with the model depicted in Fig. 6c, we propose that

Fig. 5

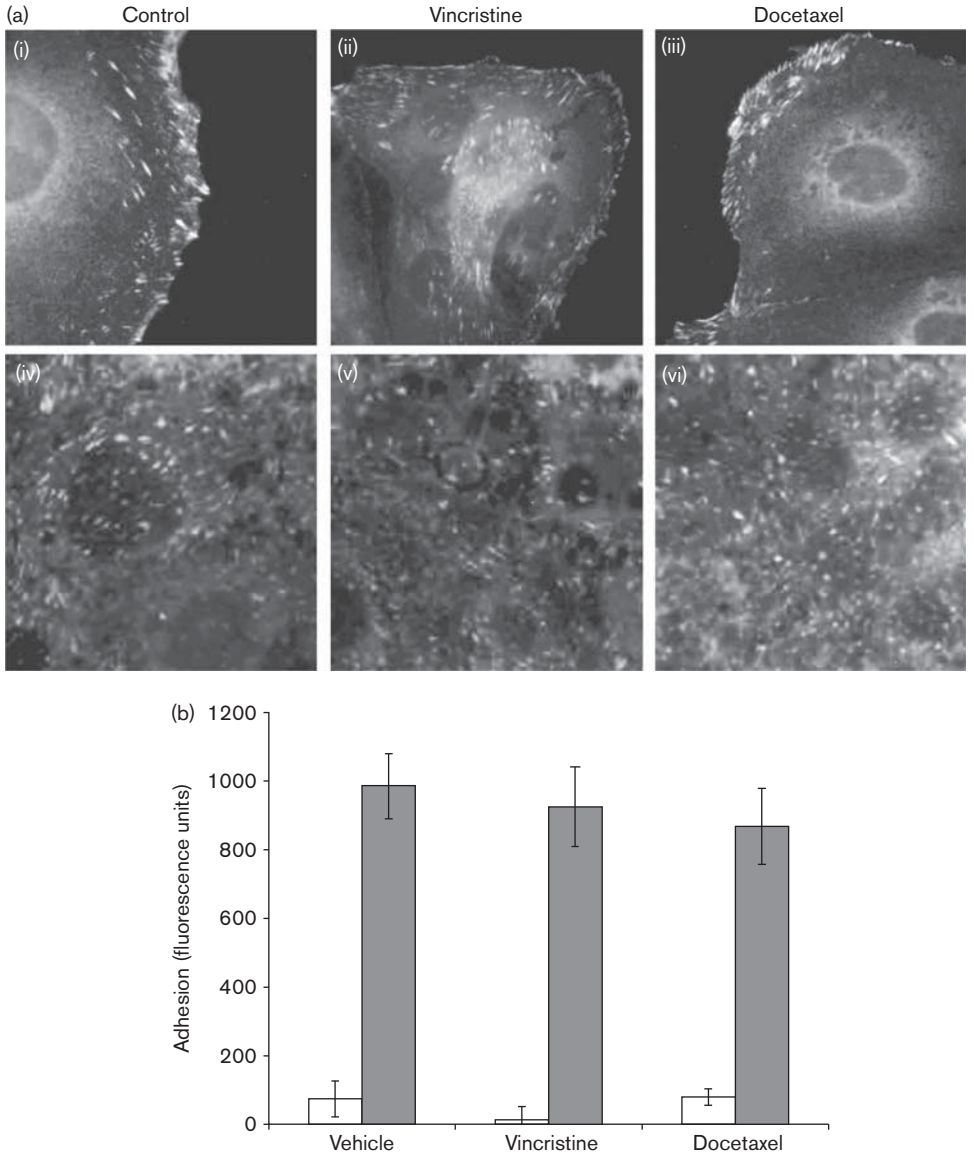

Cell–matrix adhesion. (a) Sub-confluent (i–iii) or confluent (iv–vi) Caco-2 cells were incubated (for 60 min) in either the presence or absence of the indicated compounds (10 μmol/l). Then, cells were fixed and stained with mouse anti-vinculin antibody followed by rhodamine-labeled anti-mouse IgG secondary antibody. (b) Caco-2 cells were labeled with 2′,7′-bis- (2-carboxyethyl)-5-(and-6)-carboxyfluorescein-acetoxymethyl ester, treated in the presence or absence of the drugs (10 μmol/l), 0.5 mmol/l $MnCl_2$ and/or dimethyl sulphoxide (1 : 1000; vehicle). Subsequently, 50 000 cells were plated into wells that had been coated with 2.5 μg/ml of fibronectin. As a control for non-specific adhesion, cells were also added to wells that had not been coated with fibronectin (blank wells). After incubating cells (for 60 min at 37°C), wells were washed, and cell adhesion was quantified. Values are expressed in arbitrary units (after subtracting the average blank value from each measurement) and are mean ± standard error of the mean from a representative experiment performed in six replicates. White column, control; grey column, manganese.

taking into account both the cellular context and junction dynamics may help to explain some of the apparent discrepancies that emerge when one tries to draw general conclusions from different experimental assays (e.g. the effect of vincristine on cell–cell junction morphology and its lack of effect on TEER measurements). Specifically, the model shows that junction strength increases gradually during the relatively slow phase of junction maturation, when sparse cells become sub-confluent and then confluent (on a timescale of days). Then, after reaching confluence, junction strength declines and increases abruptly, during the rapid phases of experimentally induced opening and resealing of the junctions (on a timescale of minutes and hours, respectively). In this framework, it seems that the ability of vincristine to affect junction morphology (as detected in sub-

Fig. 6

(a)

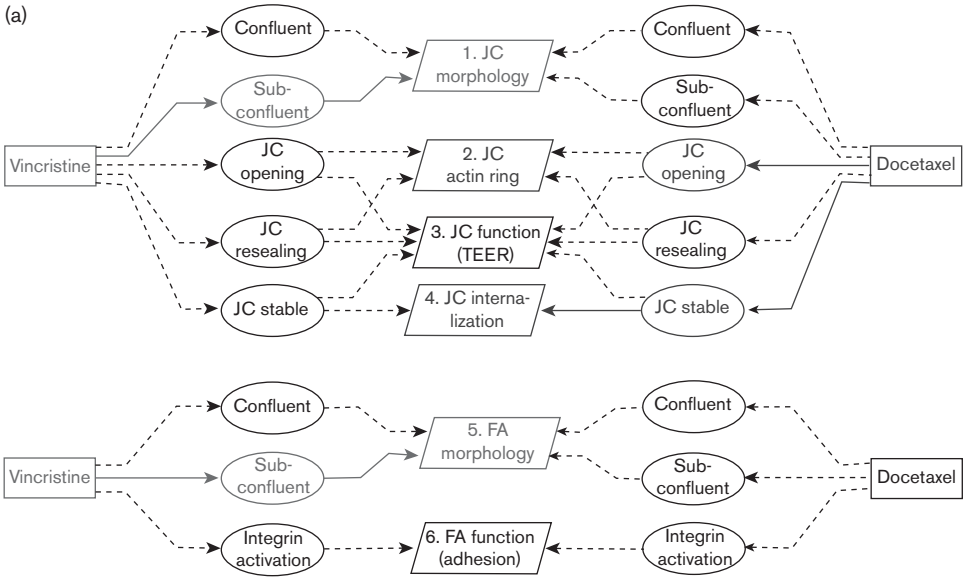

(b)

If	And if	Then
Vincristine	Cells are sub-confluent	JC morphology is affected
	JC are opened/resealed	JC function (TEER), actin ring, and JC internalization are unaffected
Docetaxel	JC are opened	JC actin ring formation is reduced
	JC are stable	JC internalization is increased
Vincristine	Cells are sub-confluent	FA morphology is affected
	Integrins are activated	FA function (adhesion) is unaffected

(c)

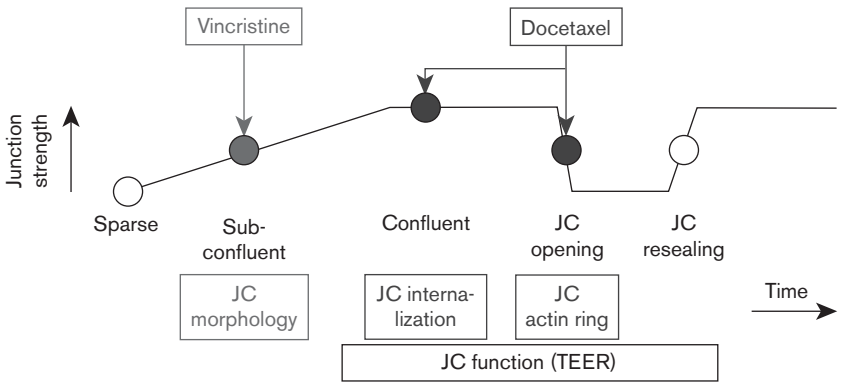

Overview. (a) The figure represents schematically the combinations of microtubule (MT)-targeting drugs (rectangles), cell contexts (ovals), and measured outcomes (parallelograms) that have been examined here. Solid lines represent the combinations that have resulted in morphological or functional changes in response to vincristine and docetaxel. Black dotted lines represent neutral combinations. In (b), a summary is also provided in an 'if, and if, then' format of conditional statements. In (c), the effects of MT-targeting drugs are correlated with the dynamic changes in junction strength that characterize different cellular contexts of confluency. FA, focal adhesions; JC, junctional complex; TEER, transepithelial electrical resistance.

confluent cells) may not easily translate into the inhibition of TEER, as TEER is measured either in confluent cells or in cells undergoing rapid opening and resealing of the junctions. Similarly, the high degree of junction strength (in confluent cells) may easily overshadow the consequences (e.g. on stable TEER) of the docetaxel-dependent increase of JAM-A internalization. Again, the rapid decrease of junction strength (on junction opening) may overshadow the consequences (e.g. on the declining phase of dynamic TEER) of the docetaxel-dependent inhibition of actomyosin ring formation. Analogous considerations may account for the discrepancy between the

effect of vincristine on cell–matrix junction morphology and its lack of effect on cell–matrix adhesion. In this case, the vincristine-dependent effect on FA morphology (as detected in sub-confluent cells) may no longer be evident in the functional evaluation of the cell adhesion assay, which deploys cell suspensions derived from confluent cells and strong integrin activation with manganese.

In conclusion, collectively, these data and considerations draw attention to the need for a comprehensive and system-level evaluation of cell contexts and junction dynamics, when analyzing the effect of drug treatments even in apparently simple and highly controlled in-vitro assays.

Acknowledgement

Work in GB laboratory was supported in part by the Negri-Weizmann Foundation.

References

1 Paris L, Tonutti L, Vannini C, Bazzoni G. Structural organization of the tight junctions. *Biochim Biophys Acta* 2008; **1778**:646–659.
2 Hartsock A, Nelson WJ. Adherens and tight junctions: structure, function and connections to the actin cytoskeleton. *Biochim Biophys Acta* 2008; **1778**:660–669.
3 Garrod D, Chidgey M. Desmosome structure, composition and function. *Biochim Biophys Acta* 2008; **1778**:572–587.
4 Geiger B, Bershadsky A, Pankov R, Yamada KM. Transmembrane crosstalk between the extracellular matrix–cytoskeleton crosstalk. *Nat Rev Mol Cell Biol* 2001; **2**:793–805.
5 Thiery JP. Epithelial–mesenchymal transitions in tumour progression. *Nat Rev Cancer* 2002; **2**:442–454.
6 D'Souza-Schorey C. Disassembling adherens junctions: breaking up is hard to do. *Trends Cell Biol* 2005; **15**:19–26.
7 Krendel M, Zenke FT, Bokoch GM. Nucleotide exchange factor GEF-H1 mediates crosstalk between microtubules and the actin cytoskeleton. *Nat Cell Biol* 2002; **4**:294–301.
8 Verin AD, Birukova A, Wang P, Liu F, Becker P, Birukov K, *et al.* Microtubule disassembly increases endothelial cell barrier dysfunction: role of MLC phosphorylation. *Am J Physiol Lung Cell Mol Physiol* 2001; **281**:L565–L574.
9 Birukova AA, Smurova K, Birukov KG, Usatyuk P, Liu F, Kaibuchi K, *et al.* Microtubule disassembly induces cytoskeletal remodeling and lung vascular barrier dysfunction: role of ρ-dependent mechanisms. *J Cell Physiol* 2004; **201**:55–70.
10 Mehta D, Malik AB. Signaling mechanisms regulating endothelial permeability. *Physiol Rev* 2006; **86**:279–367.
11 Yanagisawa M, Kaverina IN, Wang A, Fujita Y, Reynolds AB, Anastasiadis PZ. A novel interaction between kinesin and p120 modulates p120 localization and function. *J Biol Chem* 2004; **279**:9512–9521.
12 Krylyshkina O, Kaverina I, Kranewitter W, Steffen W, Alonso MC, Cross RA, *et al.* Modulation of substrate adhesion dynamics via microtubule targeting requires kinesin-1. *J Cell Biol* 2002; **156**:349–359.
13 Ivanov AI, Nusrat A, Parkos CA. Endocytosis of the apical junctional complex: mechanisms and possible roles in regulation of epithelial barriers. *Bioessays* 2005; **27**:356–365.
14 Gorovoy M, Niu J, Bernard O, Profirovic J, Minshall R, Neamu R, *et al.* LIM kinase 1 coordinates microtubule stability and actin polymerization in human endothelial cells. *J Biol Chem* 2005; **280**:26533–26542.
15 Hood JD, Cheresh DA. Role of integrins in cell invasion and migration. *Nat Rev Cancer* 2002; **2**:91–100.
16 Aldridge BB, Burke JM, Lauffenburger DA, Sorger PK. Physicochemical modelling of cell signalling pathways. *Nat Cell Biol* 2006; **8**:1195–1203.
17 Hopkins AL. Network pharmacology: the next paradigm in drug discovery. *Nat Chem Biol* 2008; **4**:682–690.
18 Bazzoni G, Martinez-Estrada OM, Orsenigo F, Cordenonsi M, Citi S, Dejana E. Interaction of junctional adhesion molecule with the tight junction components ZO-1, cingulin, and occludin. *J Biol Chem* 2000; **275**:20520–20526.
19 Martinez-Estrada OM, Villa A, Breviario F, Orsenigo F, Dejana E, Bazzoni G. Association of junctional adhesion molecule with calcium/calmodulin-dependent serine protein kinase (CASK/LIN-2) in human epithelial caco-2 cells. *J Biol Chem* 2001; **276**:9291–9296.
20 Liu Y, Nusrat A, Schnell FJ, Reaves TA, Walsh S, Pochet M, *et al.* Human junction adhesion molecule regulates tight junction resealing in epithelia. *J Cell Sci* 2000; **113 (Pt 13)**:2363–2374.
21 Bazzoni G, Shih DT, Buck CA, Hemler ME. Monoclonal antibody 9EG7 defines a novel beta 1 integrin epitope induced by soluble ligand and manganese, but inhibited by calcium. *J Biol Chem* 1995; **270**:25570–25577.
22 Fanning AS, Ma TY, Anderson JM. Isolation and functional characterization of the actin-binding region in the tight junction protein ZO-1. *Faseb J* 2002; **16**:1835–1837.
23 Ivanov AI, McCall IC, Babbin B, Samarin SN, Nusrat A, Parkos CA. Microtubules regulate disassembly of epithelial apical junctions. *BMC Cell Biol* 2006; **7**:12.
24 Bazzoni G, Dejana E. Endothelial cell-to-cell junctions: molecular organization and role in vascular homeostasis. *Physiol Rev* 2004; **84**:869–901.
25 Papini E, Satin B, Norais N, de Bernard M, Telford JL, Rappuoli R, *et al.* Selective increase of the permeability of polarized epithelial cell monolayers by Helicobacter pylori vacuolating toxin. *J Clin Invest* 1998; **102**:813–820.
26 Martinez-Palomo A, Meza I, Beaty G, Cereijido M. Experimental modulation of occluding junctions in a cultured transporting epithelium. *J Cell Biol* 1980; **87**:736–745.
27 Ivanov AI, McCall IC, Parkos CA, Nusrat A. Role for actin filament turnover and a myosin II motor in cytoskeleton-driven disassembly of the epithelial apical junctional complex. *Mol Biol Cell* 2004; **15**:2639–2651.
28 Bazzoni G, Hemler ME. Are changes in integrin affinity and conformation overemphasized? *Trends Biochem Sci* 1998; **23**:30–34.
29 Van der Sandt IC, Gaillard PJ, Voorwinden HH, de Boer AG, Breimer DD. P-glycoprotein inhibition leads to enhanced disruptive effects by anti-microtubule cytostatics at the in-vitro blood-brain barrier. *Pharm Res* 2001; **18**:587–592.
30 Palazzo AF, Gundersen GG. Microtubule–actin crosstalk at focal adhesions. *Sci STKE* 2002; **2002**:pe31.
31 Bazzoni G, Tonetti P, Manzi L, Cera MR, Balconi G, Dejana E. Expression of junctional adhesion molecule-A prevents spontaneous and random motility. *J Cell Sci* 2005; **118**:623–632.
32 Deschesnes RG, Patenaude A, Rousseau JL, Fortin JS, Ricard C, Cote MF, *et al.* Microtubule-destabilizing agents induce focal adhesion structure disorganization and anoikis in cancer cells. *J Pharmacol Exp Ther* 2007; **320**:853–864.